Supplementary Information for

Intensified cross-linking dramatically improved mechanical properties of hydroxyapatite and cellulose composites for repairing bone segmental defects

Qingyou Liang,[ab] Jie Dong, ‡[c] Jian Ren,[a] Cairong Xiao[a] and Chunlin Deng*[a]

[a] *School of Materials Science and Engineering, South China University of Technology, Guangzhou 510640, China*

[b] *Analytical and Testing Center, South China University of Technology, Guangzhou 510640, China*

[c] *Department of Radiation Oncology, The Third Affiliated Hospital of Sun Yat-sen University, Guangzhou 510630, China*

S1. Characterization of the raw materials

The composite material was mainly composed of hydroxyapatite (HA) and cellulose fibril (CF), which originated from the raw materials including quantitative filter paper, calcium hydroxide ($Ca(OH)_2$) and pure phosphatic acid (H_3PO_4). Their Fourier transform infrared (FT-IR) spectra were shown in Figure S1, in which all the main peaks can be easily assigned. It is noticeable that the peak at 2900 cm^{-1} in the spectrum of filter paper (Figure S1a) was assigned to CH_2 vibration, by which CF can be confirmed in the composite material.

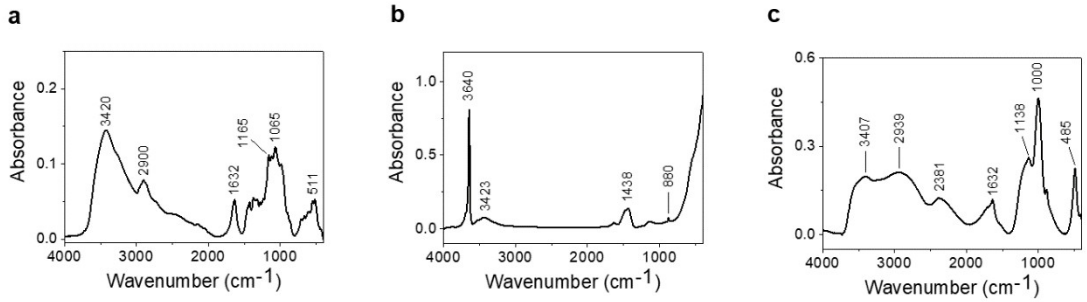

Fig. S1 The FT-IR spectra of the quantitative filter paper (**a**), $Ca(OH)_2$ (**b**) and pure H_3PO_4 (**c**).

The quantitative filter paper was tested by energy dispersive spectroscopy (EDS) and $Ca(OH)_2$ was tested by electron probe X-ray micro-analyzer (EPMA) (Figure S2a, b). The C element in $Ca(OH)_2$ came from the conductive adhesive. The morphology of CF was characterized by SEM (Figure S2c), which showed that the diameter of CF was 10–20 μm and some of the fibers was uncurled to form a plane.

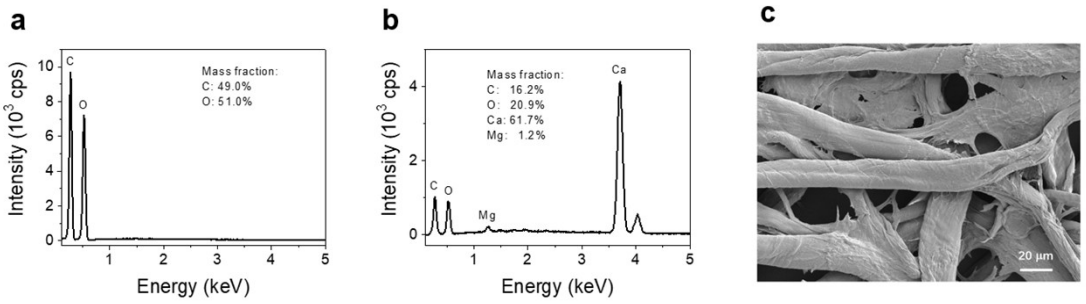

Fig. S2 The EDS spectrum of the quantitative filter paper (**a**) and EPMA spectrum of $Ca(OH)_2$ (**b**) and SEM morphology of CF (**c**).

Pure HA and dicalcium phosphate dihydrate (DCPD) were also characterized by FT-IR spectroscopy and the spectra were shown in Figure S3, which was used as a reference

to analyze the components in the material.

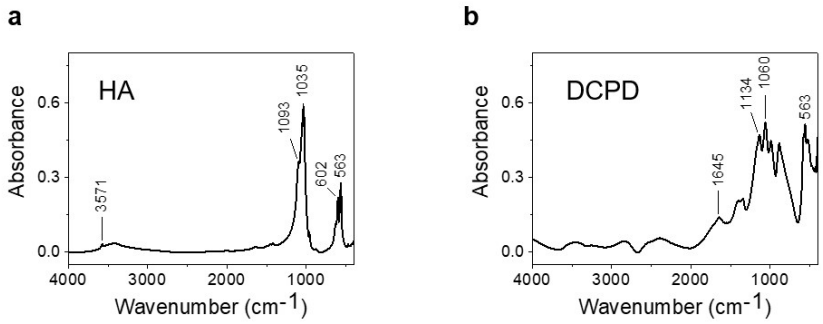

Fig. S3 The FT-IR spectra of pure HA (**a**) and DCPD (**b**).

S2. Characterization of the intermediate products

Regulating the pH in neutralization reaction was important for the final product. The pH value should reach 13~14 to obtain HA. If the pH value was 10~11, DCPD formed in the material, instead of HA (Figure S4). It is necessary to keep monitoring pH in the reaction process. FT-IR and X-ray diffraction (XRD) spectroscopy were employed.

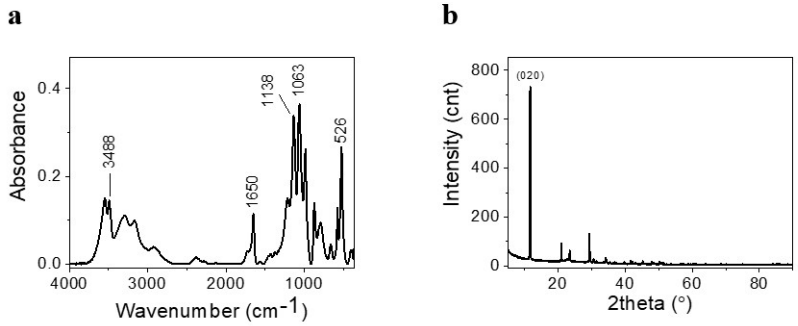

Fig. S4 Characterization of the intermediate products under pH of 10~11: FT-IR (**a**) and XRD (**b**).

After the neutralization with $Ca(OH)_2$, the particle size was analyzed by dynamic light scattering (DLS) with 532 nm laser and the dispersive solvent of absolute ethanol. DLS showed that the average size of particles in the suspension was 92 μm (Figure S5a), which would emerge under pressure. CF was obtained by means of hydrolysis of the filter paper fiber with 75%(V/V) H_3PO_4 and thus was of negative charges on the surface. Zeta potential of pure CF was -11.8 mV (Figure S5b), which demonstrated that CF was able to be combined with HA by electrostatic interaction. Ionic bonds will form and enhance the cross-linking between HA and CF.

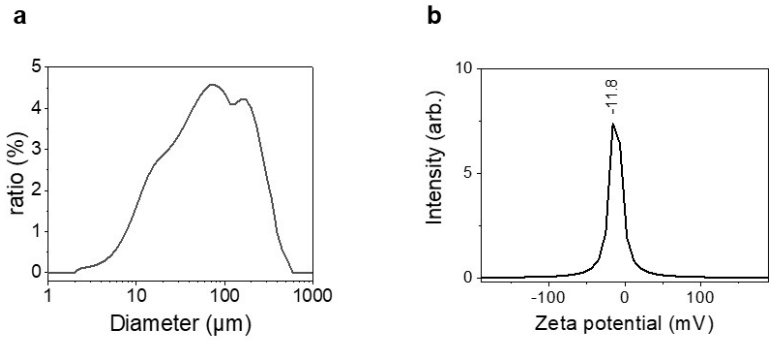

Fig. S5 The size distribution of particles in the suspension after the neutralization reaction with $Ca(OH)_2$ (**a**) and the Zeta potential of pure CF (**b**).

S3. Characterization of the final products

EDS mapping for the final product was performed for individual elements, including C, P, Ca, et al (Figure S6). All the elements were distributed uniformly.

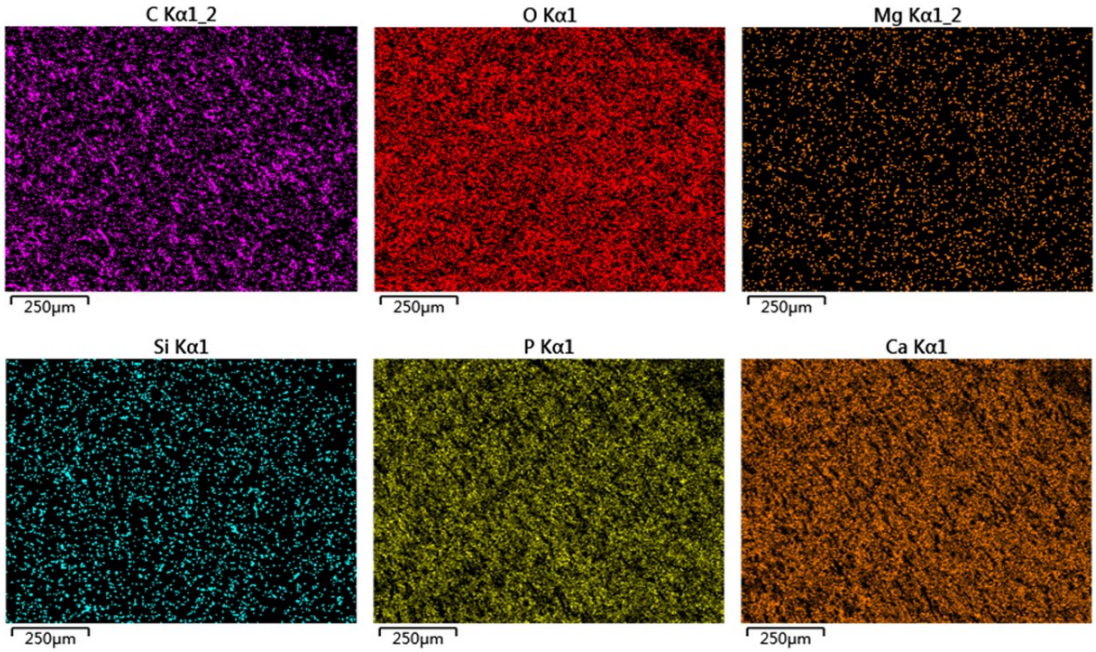

Fig. S6 EDS mapping of the individual elements.

In XRD pattern, peaks were fitted to calculate the degree of crystallinity and full width at half maximum (FWHM) (Figure S7). According to Figure S7b, the crystallinity of HA was 83.4% and according to Figure S7c, the crystallinity of CF was 83.4% and that of CF was 73.4%. This was consistent with the results that HA and CF had been combined together with the depth of 20–30 nm. In the combination area of HA and collogen in natural bone, HA was non-crystalline.[1] Similar reason may occur

in this hybrid material and the contractile stress was generated in this structure.[2] Scherrer Equation can be employed to calculate the size of crystallite (D_{hkl}) on the given crystalline surface:

$$D_{hkl} = \frac{K\lambda}{B_{hkl}\cos\theta} \quad \text{(Equation 1)}$$

Where K is the shape factor (K=0.9 is a proper estimation), λ is the wavelength of X-ray (0.15406 nm), B_{hkl} is FWHM of the diffraction peak. Perpendicular to the surface (002), there was the largest crystallite as 16.92 nm, which revealed that HA may tend to grow along c axis.

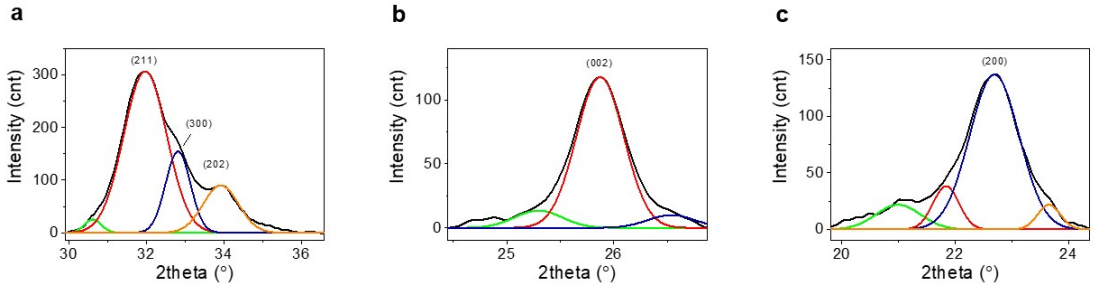

Fig. S7 Fitted XRD peaks for HA (**a**, **b**) and CF (**c**).

To further investigate the cross-linking of inorganic and organic phases on the macroscopic scale, infrared microscopy (IRM) mapping was utilized. As there were restrictions for IRM testing, a model material was prepared. One drop of pure CF suspension was added to the surface of the monocrystalline silicon. Then 1 μL of H_3PO_4 and $Ca(OH)_2$ suspension were added into CF consequently to react and form mineral phase. The aperture of IRM was set as 100 μm and an area of 1.3 mm×0.7 mm was selected. Figure S8a presented the optical morphology of the sample, which showed that CF was arranged as grids and mineral phase filled the gap of network. In IRM mapping (Figure S8b), 2903 cm^{-1} was selected because it's C-H vibration and only existed in the spectrum of CF. The unit of color scale bar was reflectance—that was just transmittance. The lower the reflectance was, the higher the CF content. The red and yellow colors in Figure S8b approximately formed a grid similar to Figure S8a, which meant that the mineral phase formed in the gap of CF networks on the millimeter scale.

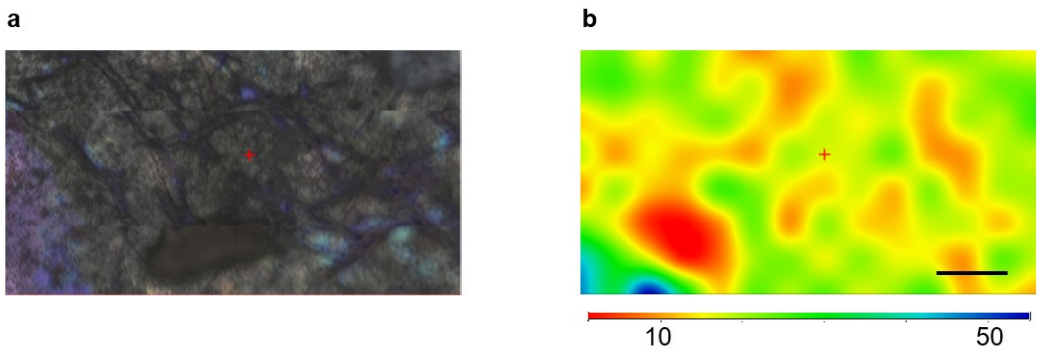

Fig. S8 IRM mapping for the model hybrid material. (**a**) The optical microscopy. (**b**) The chemical mapping according to 2903 cm^{-1} peak that represented CF (the scale bar: 200 μm).

In the Raman analysis of the water peak in the material, the same laser should be consistently designated for all the samples, because different lasers create different Raman spectrum. Figure S9 showed that Raman spectra had distinct discrepancy between 532 and 633 nm lasers (without fitting). Considering fluorescence, 633 nm was selected in this experiment.

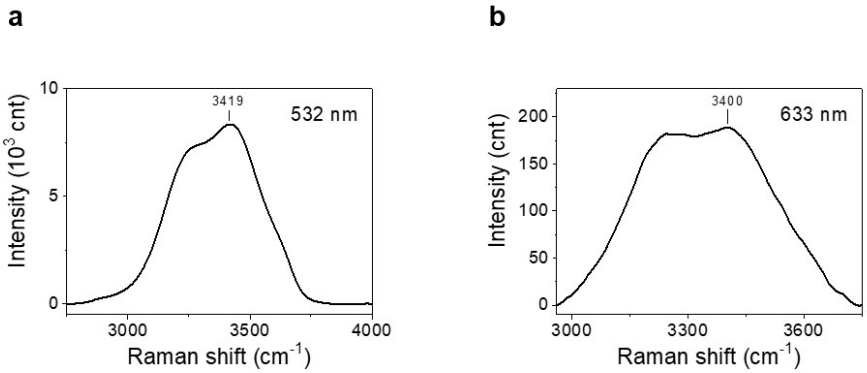

Fig. S9 Original Raman spectra of water under 532 nm (**a**) and 633 nm (**b**).

S4. Surface tension calculation

We put the hybrid material in the water and found that it seemed "hung" under the water surface (Figure S10). The reason was that the water had surface tension. According to the force equilibrium, we can get:

$$f \sin\theta = mg - \rho_0 gV \qquad \text{(Equation 2)}$$

where θ is the contact angle of the water and material, m is the mass of the material, ρ_0 is the water density and V is the volume of the material. The force f was generated by the surface tension γ and determined by:

$$f = \gamma C \qquad \text{(Equation 3)}$$

where C is perimeter of the material. With combination of the two equations, we obtain $\gamma = 0.3649$ N m^{-1} (25℃). The material had a high-energy surface because γ was higher than 0.1 N m^{-1}. This may explain why there was strong cross-linking inside the material.

Fig. S10 The composite material seemed “hung” under the water surface owing to the surface tension. The volume of the beaker was 20 mL.

S5. HE stain results

Hematoxylin and eosin (HE) stain was also performed (Fig. S11), whose results were similar to that of Masson stain. In the control group, the heterotopic ossification occurred and the trabecular bone lost connection, which revealed that the tibia had underwent excessive load. Conversely, the implanted group showed the normal tibia. Therefore, implanting material was very important for BSD repair.

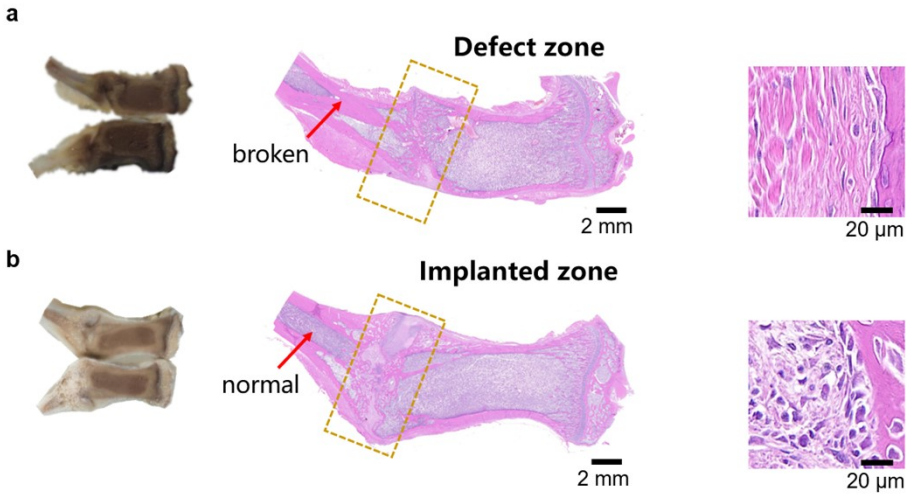

Fig. S11 Hematoxylin and eosin (HE) stain results: **a,** The control group. **b,** The implanted group. The scale bars in the middle figures are 2 mm, while the scale bars in the right figures are 20 μm.

S6. Discussion about cracks of the material in application

Although our composite material has low porosity and no big pores before use, cracks with large size will appear when the composite material is soaked in water *in vitro* or implanted *in vivo*, thus providing enough space for cell growth.

The change of the cracks of the sample soaked in water with different timespan were shown in Fig. S12. In all the timespans, there was one main crack, and one or more minor crack(s). Main crack went through the surface of the sample, while minor cracks were shorter and narrower. A crack appeared immediately after the material was soaked for 10 min, which showed that the material could interact with water quickly. At 10 min of soaking, the depth of the main crack was 1046±248 μm. The size of the sample on the direction of the depth of the crack was about 4 mm, which meant that the sample was still entire. At 1 hour of soaking, the depth of the main crack was 1093±380 μm. At 1 day of soaking, the depth of the main crack was 1057±270 μm. The results revealed that within one day, the depth of the crack was about 1 mm and didn't change significantly ($p >> 0.05$). In addition, the width of the crack was less than 100 μm at this moment.

At 1 week of soaking, the depth of the main crack was 1235±75 μm that was larger than before, while the width of the crack increased to 100~200 μm. The surface of the sample began to be rough. At 35 days (about 1 month) of soaking, the depth of the main crack was 1514±188 μm, which was significantly larger than that of 1 day and 1 week ($p < 0.05$). The width of the crack maintained at 100~200 μm. At the same time, the number of minor cracks increased to three and the surface of the sample became rougher. In summary, the crack formed quickly when the material was put in water, but developed slowly. It was very important that these cracks provide enough space for cells to grow. Therefore, the material was able to work as a "scaffold".

To investigate the function of the crack, cell culture on the sample surface was carried out *in vitro*. Fig. S13 showed that the mouse bone mesenchymal stem cells (mBMSCs) (colored green) were able to grow and spread on the surface of the material. The area between the parallel yellow lines were a crack, where mBMSCs was also able to enter and grow. The depth of the crack was 1~1.5 mm, the length was 1 mm, and the width

was 150 μm. Therefore, the crack actually became a vast cavity that allowed mBMSCs to move and exchange matter and energy. Or to say, the crack could accommodate mBMSCs as a scaffold and meet the requirements of cell proliferation.

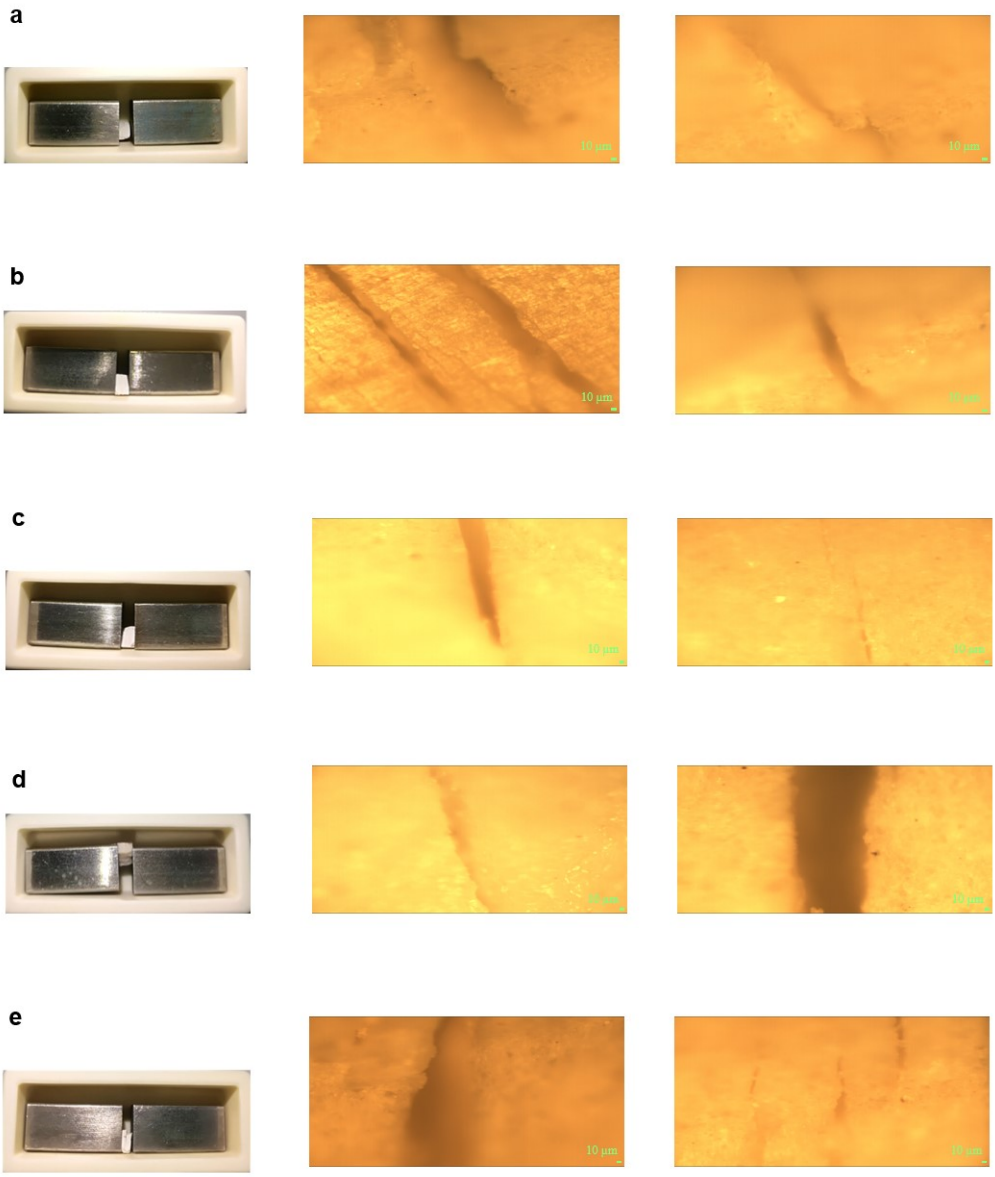

Fig. S12 The cracks on the surface of the composite material with different soaking timespan: **a,** Soaking for 10 min. **b,** Soaking for 1 h. **c,** Soaking for 1 day. **d,** Soaking for 1 week. **e,** Soaking for 35 days (5 weeks). The outer size of the crucible is 5 cm×2 cm. The scale bars are all 10 μm.

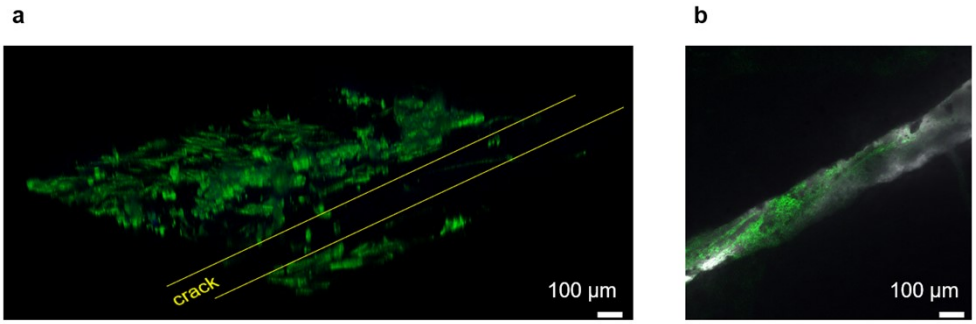

Fig. S13 The observation of mBMSCs proliferation on the material surface: **a,** Upon the surface of the material. **b,** Inside the crack. The scale bars are all 100 μm.

The crack was also observed in the implantation experiment *in vivo* (Fig. S14), which formed after the composite material contacted with body fluid of the rat. This phenomenon was consistent with that of the *in vitro* study. The result demonstrated that cells were able to grow and proliferate upon and inside the implanted material, which was beneficial to osteogenesis.

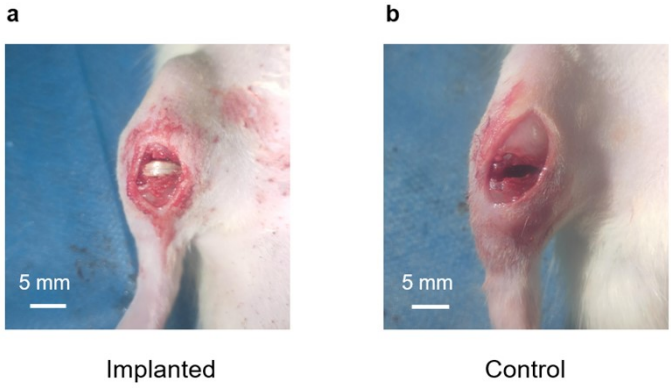

Fig. S14 The photos of surgery scenes: **a,** Implanted group. **b,** Control group. The scale bars are all 5 mm. A crack can be seen in **a**.

S7. The Bioactivity test using SBF and FCS

The bioactivity test was performed in a simulated body fluid (SBF) and a fast mineralization solution (FCS), respectively, following the two references.[3,4] The results are shown in Fig. S15. SEM image of the original sample is shown in Fig. S15a. With SBF for 3 days (Fig. S15b), there were several small spheres formed on the material surface, which showed that HA particles had precipitated. With FCS for 3 days (Fig. S15c), there were numerous HA flakes generated on the material surface. Therefore, the sample has mineralization ability.

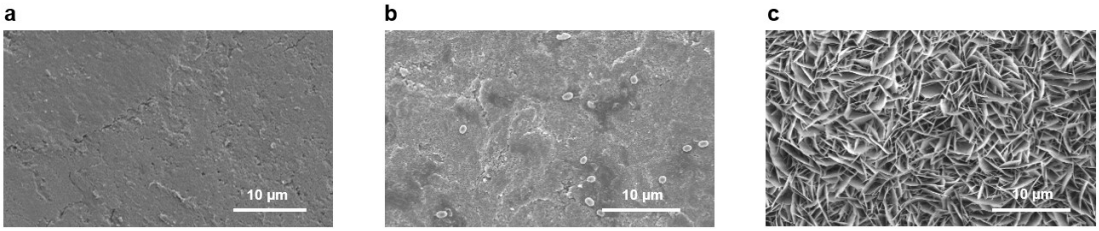

Fig. S15 The observation of the material surface in the bioactivity test for 3 days: **a,** Original. **b,** SBF. **c,** FCS. The scale bars are all 10 μm.

References

1 E. Hamed and I. Jasiuk, *Mater. Sci. Eng. R*, 2012, **73**, 27–49.

2 H. Ping, W. Wagermaier, N. Horbelt, E. Scoppola, C. H. Li, P. Werner, Z. Y. Fu and P. Fratzl, *Science*, 2022, **376**, 188–192.

3 T. Kokubo and H. Takadama, *Biomaterials*, 2006, **27**: 2907–2915.

4 W. R. Han, L. T. Liu, X. C. Wang, Z. H. He, D. Y. Yin, Y. Y. Wu, C. L. Deng, *Mater. Lett.*, 2023, **342**: 4.